J Electr Eng Technol.2015;10(1): 155-164
http://dx.doi.org/10.5370/JEET.2015.10.1.155

ISSN(Print) 1975-0102
ISSN(Online) 2093-7423

Comparison of Two Rotor Configurations by Changing the Amount of Magnet and Reluctance Components

Esra Kandemir Beser†, Sabri Camur*, Birol Arifoglu* and Ersoy Beser*

Abstract – In this paper, two rotor configurations including different amount of magnet and reluctance parts are presented. The rotors are constituted by means of a flexible hybrid motor structure. Considerable features of the hybrid structure are that the combination of the magnet and reluctance parts can be suitably modified and the mechanical angle (β) between the parts can also be varied. Two hybrid rotor configurations have been considered in this study. First, finite element (FE) simulations were carried out and the torque behaviors of the motors were predicted. The average torque (T_{avg}) and maximum torque (T_{max}) curves were obtained from FE simulations in order to find suitable β. Mathematical model of the motors was formed in terms of a,b,c variables considering the amount of the magnet and reluctance parts on the rotor and simulations were performed. Rotor prototypes, motor drive and drive method were introduced. Torque profiles of the motors were obtained by static torque measurement and loaded tests were also realized. Thus, simulation results were verified by experimental study. There is a good match between predictions and measurements. The proposed motors are operated with electrical 120° mode as a brushless DC motor (BLDC) and torque versus speed characteristics show a compound DC motor characteristic. The motors can be named as brushless DC compound motors.

Keywords: Brushless machines, Permanent magnet motors, Reluctance motors, Finite element simulations, Modelling hybrid motors, Axially laminated rotors.

Nomenclature

[V]	phase-neutral voltages matrix
[I]	phase currents matrix
[R]	resistance matrix
[L]	inductance matrix
[λ]	total flux on the phase winding
[λ_m]	total magnet flux on the phase winding
θ_r	rotor position
ω_r	angular velocity
T_e	electromagnetic torque
T_l	load torque
p	the number of pole pairs
j	inertia torque
m	ratio of the magnet part
r	ratio of the reluctance part

1. Introduction

Permanent magnet assisted synchronous reluctance machines (PMa-SynRM) have become popular machines in many applications due to having high power density, high power factor, high efficiency and wide speed range. These machine types can be called as hybrid machines since they include both reluctance and permanent magnet torques. The rotor can be designed in many different structures to provide both magnet and reluctance torques.

Various studies have been realized in the literature about PMa-SynRM. Two-part rotor configuration is introduced in [1] and analyses are realized for the hybrid motor possesses 59% reluctance part and 37% permanent magnet part. The analyses indicates that it is possible to obtain a constant-power speed range with currents greater than the rated current by setting the angle between d-axes of permanent magnet and reluctance parts to 90° [1].

A synchronous motor with two-part rotor having same properties in [1] is studied and flux weakening performance is experimentally investigated in [2]. It is represented that a two-part rotor might be composed to give an approximately constant characteristic of input power over a field-weakening speed range, with high input power factor [2].

A theoretical study based on the rotor design of a synchronous machine with two-part rotor is realized by finite element method (FEM) in [3]. According to the numerical results design parameters are determined in order to obtain an optimal design [3].

A synchronous motor with two-part rotor comprising 29% reluctance part and 67% permanent magnet part is described in [4] and [5]. Output power characteristics

† Corresponding Author: Dept. of Electrical Engineering, Kocaeli University, Turkey. (esrakandemir@kocaeli.edu.tr)
* Dept. of Electrical Engineering, Kocaeli University, Turkey. ({scamur, barif, ebeser}@kocaeli.edu.tr)
Received: April 15, 2014; Accepted: August 13, 2014

demonstrate that two-part rotors have the capability of being designed to provide good performance over a wide constant-power speed range [4, 5].

Field-weakening performance of synchronous reluctance motors (SynRM) and interior permanent-magnet (IPM) motors is compared to an induction machine in [6]. The multiple-barrier IPM motor structure shows the most promising field-weakening performance [6].

A PMa-SynRM and drive are designed for hybrid electrical vehicles in [7]. The motor prototype is composed by adding proper magnets into the flux barriers. The construction having 12 poles are found to be the best choice [7].

In [8], a FEM approach is achieved to analyze the effects of rotor design variables on four-pole transversally laminated SynRM performance. It is determined that an insulation ratio of 0.4-0.6 should be selected to maximize the developed torque. A comparison between the effect of the concentric winding and distributed winding is performed considering the overall performance of the PMa-SynRM [8].

Two PMa-SynRMs are studied by gluing axially-laminated iron and two different magnet materials in [9]. It is indicated that very poor maximum energy product PM material should not be chosen for application that requires high power density [9].

Slot effect in PMa-SynRMs is analyzed and verified by experiments in [10]. Three different type PMa-SynRMs are studied. The results show that the teeth harmonics can be reduced by both more layers and stator slot skewing [10].

A four-pole IPM motor prototype including NdFeB magnets into the transversally laminated layers is used in [11] in order to investigate cross-saturation effects in IPM motors and impacts on sensorless control [11].

A motion-sensorless control of a PMa-SynRM is realized in [12]. Experimental machine is an eight-pole transversally laminated design having four flux barriers per pole and magnets in three flux barriers [12].

The study in [8] is improved and a FEM approach is utilized to analyze the effects of rotor design variables on SynRM performance in [13]. The lengths of tangential and radial ribs affect the developed torque significantly and use of small magnets in the rotor is recommended to saturate these ribs and improve the performance of the SynRM. Effects of the magnets on d–q inductances are examined and output torque of SynRM and PMa-SynRM is compared [13].

A design having flexible magnets between transversally laminated layers is proposed in [14] and dynamic control of the PMa-SynRM is realized [14].

An analytical model for a PMa-SynRM with four flux barriers per pole is presented in [15]. The machine designer can place the magnets anywhere in the flux-barriers by the model. Improvement of the motor performance due to the permanent magnets is also easily included in the Eqs. [15].

In [16], an effective torque ripple reduction in SynRM and PMa-SynRM is carried out by designing flux barriers of different geometries. Two motor prototypes are built and tested. The torque ripple becomes about one-third of that produced by the classical IPM rotor design at nominal current [16].

Various designs of reluctance machines are discussed in [17]. FEM is performed to simulate and calculate flux distribution. Permanent magnet materials are added for improving the saliency ratio. The use of permanent magnets is exhibited to improve rotor saliency ratio and hence the motor performance [17].

The effect of PM volume on the PMa-SynRM is analyzed in [18], although lamination geometry and stack length are kept fixed. The influence of the PM volume on the machine performance is highlighted by FE simulations and measurements [18].

An analytical procedure is presented in [19] in order to reduce the magnet quantity in PMa-SynRMs without affecting the torque versus speed performance. The theoretical formulation is verified with FEA approach and experiments on a prototype machine [19].

When mentioned studies about PMa-SynRMs in the literature are examined, it is seen that they include improving new designs, modeling the designs, controlling the machines, sensorless operating and improving the features and control methods of the existing configurations. Popular PMa-SynRM configurations in the literature can be generally described as the rotors made of axially laminated layers with added flexible permanent magnet material between the layers, the designs having permanent magnets into the flux barriers on transversally laminated layers and two part structures having constant ratio and position between magnet and reluctance parts. The common point for the presented motor types is their operation with the principles of synchronous machines.

Regarding to the interest for the PMa-SynRMs, the main purpose of this paper is to compare two hybrid rotors by means of a flexible hybrid motor structure allowing the modification of magnet and reluctance components on the rotor. The significant features of the hybrid motor are that the hybridization ratio is modified by the magnet and reluctance components, the angle between the components can be varied and drive method bases on the operation of a brushless DC motor (BLDC). The proposed rotors are presented in Section 2. The designs are first studied by a set of FEA in Section 3 and then simulations are carried out in Section 4. In Section 5, produced rotors and motor drive are introduced and drive method is explained. Static torque tests and loaded tests are realized and results are presented. Finally, the results of the complete study are presented in Section 6.

2. Proposed Rotor Structures

Proposed rotors consist of two independent sections as

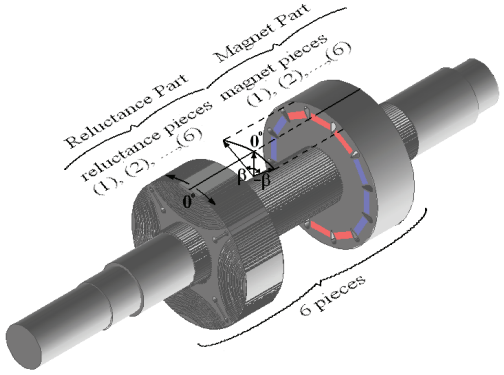

Fig. 1. Principle sketch of the hybrid rotor

magnet and reluctance parts. They are provided by a flexible hybrid rotor configuration [20, 21]. In the hybrid rotor structure, the parts are configured by means of magnet and reluctance pieces.

Six magnet and six reluctance pieces are manufactured in order to achieve different hybrid rotor types. Totally, six pieces can be arranged on the rotor shaft. Principle sketch of the hybrid rotor structure is shown in Fig. 1.

As it can be seen from Fig. 1 that five hybrid rotor types can be constructed by this flexible structure. Completely magnet and reluctance rotors can be also obtained by using six magnet and six reluctance pieces.

Another significant feature for the hybrid rotor configuration is that the position of the parts can be changed with respect to each other by 5 mechanical degrees due to the suitable structure of the pieces and shaft. Therefore, the effect of different angle values between the parts can be studied. The mechanical angle between the parts is defined as β. Two hybrid rotor configurations have been considered in this paper. Studied rotors are given in Table 1.

Table 1. Proposed rotors according to numbers of the magnet and reluctance pieces

Number of Magnet Pieces	Number of Reluctance Pieces	Motor Name
2	4	Hybrid A
4	2	Hybrid B

NdFeB magnets have been preferred for the magnet part and axially laminated rotor has been built for the reluctance part. The machine has four poles and the generated torque includes both magnet and reluctance torques. Stator skew angle is determined as 15° (mechanical) considering the torque profiles obtained by FE simulations in point of ripple and maximum value of the profile. The remarkable dimensions and specifications of the stator and rotors are given in Table 2.

3. Finite Element Simulations

In order to analyze the proposed rotor designs, first, models of the rotor and stator structures are formed according to the design parameters in Table 1. After the motors have been modeled, FE method is performed for the analysis of two rotor designs. Two-dimensional FE package is used to determine the torque acting on the rotor.

In FE simulations, constant currents of 10A, 20A and 40A were applied to two stator windings respectively, considering electrical 120° operation mode. The step for each simulation was chosen as 5 mechanical degrees. The angle β was also varied in the range of -50° to 15°. The torque waveforms were obtained by means of FE method according to variable β values and different currents for Hybrid A and Hybrid B. Some FE results of the torque profiles in the hybrid motors are presented in Fig. 2 at electrical 120° operation mode for different β values (I= 20A).

In order to determine the suitable β for the hybrid motors, the average torque (T_{avg}) and the maximum torque (T_{max}) can be obtained from the output torque profiles. T_{avg} is calculated for electrical 120° operation mode, T_{max} is calculated to prepare the preliminary study for controlling of the motors. Since the torque profiles were obtained for variable β and current values, 3-D graphs were formed to evaluate the existing data. T_{avg} and T_{max} curves related to β and current are shown in Fig. 3 for Hybrid A and Hybrid B.

It is seen from Fig. 3 that that at low currents, β does not affect the T_{avg} and T_{max} values so much. However, β becomes a remarkable parameter by the increase of the

Table 2. The remarkable dimensions and specifications of the hybrid motor

Stator			
Outer diameter	200mm	Stack length	240mm
Inner diameter	125mm	Number of slots	36
Number of poles	4	Winding	Distributed
Lamination	M400-50A	Stator skewing angle	15°(mechanical)
Rated Power 10 kW Rated Speed 1900 rpm Torque 50 Nm			
Rotors			
Magnet Part		Reluctance Part	
Diameter	123.9mm	Diameter	124.3mm
Magnet type	NdFeB	Magnetic material	Grain oriented M6
Rotor material	Steel 1010	Magnetic material thickness	1mm
Magnet thickness	5mm	Non-magnetic material	Aluminum
		Non-magnetic material thickness	1mm

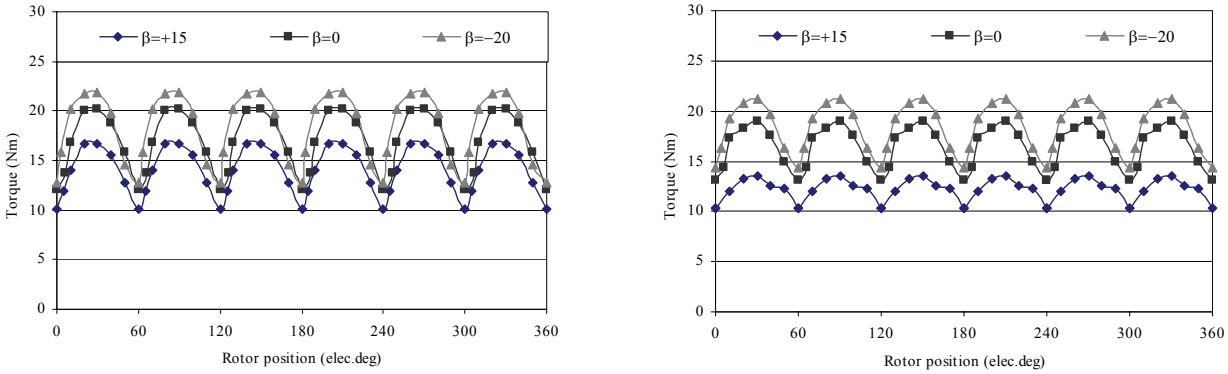

Fig. 2. Simulated torque behaviors as a function of the rotor position for different β values in the (a) Hybrid A (b) Hybrid B (I=20A)

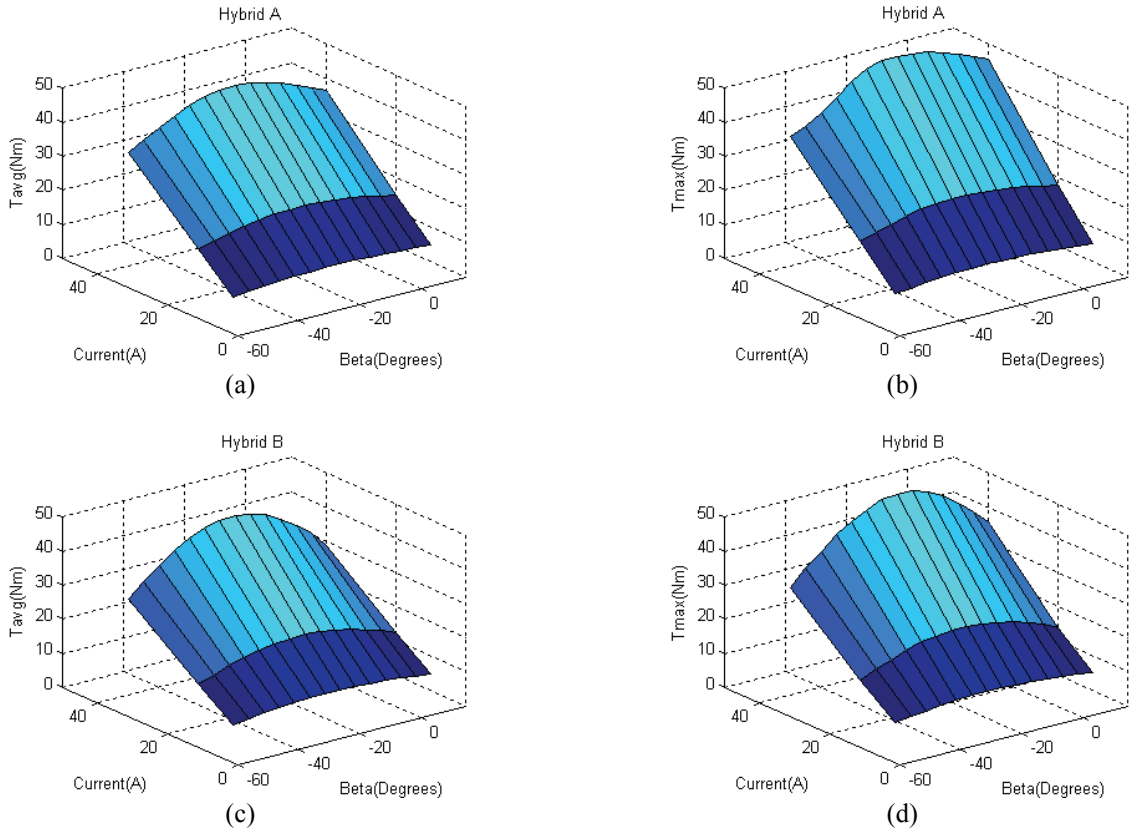

Fig. 3. Analysis results of T_{avg} (a), (c) and T_{max} curves (b), (d) as a function of β and current for Hybrid A and Hybrid B

current. The concentrated regions of the 3-D graphs for the hybrid motors were determined and acceptable β ranges were obtained for T_{avgmax} and T_{max} values by using results. Acceptable β value is determined in the range of -20° and -10° for the hybrid motors considering FE results.

4. Mathematical Model and Simulations of Hybrid Motors

Mathematical model of the hybrid motors are formed in terms of a, b, c phase variables. Both magnet and reluctance machine models exist in the model. To complete the hybrid motor model it is important to combine two mathematical models considering the hybridization on the rotor. The voltage equations of the hybrid machine can be obtained by the following equation systems.

By changing the values of m and r, the equations of the machine model are modified and the motor acquires a different structure.

$$[V]_{a,b,c} = [R]_{a,b,c}[I]_{a,b,c} + \frac{d}{dt}[\lambda]_{a,b,c} \quad (1)$$

$$[\lambda]_{a,b,c} = \left(m[L_m]_{a,b,c} + r[L_r]_{a,b,c}\right)[I]_{a,b,c} + m[\lambda_m]_{a,b,c} \quad (2)$$

$$[V]_{a,b,c} = [R]_{a,b,c}[I]_{a,b,c} + \frac{d}{dt}\left\{\left(m[L_m]_{a,b,c} + r[L_r]_{a,b,c}\right)[I]_{a,b,c} + m[\lambda_m]_{a,b,c}\right\} \quad (3)$$

$$[V]_{a,b,c} = [R]_{a,b,c}[I]_{a,b,c} + \left(m[L_m]_{a,b,c} + r[L_r]_{a,b,c}\right)\frac{d[I]_{a,b,c}}{dt} + \left(m\frac{\partial[L_m]_{a,b,c}}{\partial\theta_r} + r\frac{\partial[L_r]_{a,b,c}}{\partial\theta_r}\right)[I]_{a,b,c}\,\omega_r + m\frac{\partial[\lambda_m]_{a,b,c}}{\partial\theta_r}\omega_r \quad (4)$$

The electromagnetic torque and mechanical equations can also be written as

$$T_e = p\left\{\frac{1}{2}[I]^T_{a,b,c}\left(m\frac{\partial[L_m]_{a,b,c}}{\partial\theta_r} + r\frac{\partial[L_r]_{a,b,c}}{\partial\theta_r}\right)[I]_{a,b,c}\right\} + p\left\{[I]^T_{a,b,c}\,m\frac{\partial[\lambda_m]_{a,b,c}}{\partial\theta_r}\right\} \quad (5)$$

$$T_e - T_l = \frac{d\omega_r}{dt}\frac{j}{p} \quad (6)$$

The values of m and r variables change according to the magnet and reluctance pieces. m and r values in the studied motors are given in Table 3 for this work.

By constituting the mathematical equations, the machine model was configured in the simulation program. Stator winding resistance (R_s) was defined as 0.24 Ω for each winding. Self inductance ($L_{m(aa)}$ and $L_{r(aa)}$) and mutual inductance ($L_{m(ab)}$ and $L_{r(ab)}$) for reluctance and magnet machines were identified as a function of the rotor position as

$$L_{m(aa)}(\theta_r) = 8.4 + 2.6\cos(2\theta_r) + 0.4\sin(2\theta_r)\,mH \quad (7)$$

$$L_{m(bc)}(\theta_r) = 2.6 + 1.7\cos(2\theta_r) + 0.4\sin(2\theta_r)\,mH \quad (8)$$

$$L_{r(aa)}(\theta_r) = 12.7 + 9.8\cos(2\theta_r) - 0.8\sin(2\theta_r)\,mH \quad (9)$$

$$L_{r(bc)}(\theta_r) = -4.3 + 9.6\cos(2\theta_r) - 0.3\sin(2\theta_r)\,mH \quad (10)$$

Then, inductance matrices (L_m and L_r) were constituted for hybrid motors according to the hybridization on the rotor and included into the machine model. Inertia torque values were calculated considering the materials and dimensions of the rotors and friction was neglected. m and r values were defined as Table 3. The angle β was set to -20° and machine parameters were added into the model. An inverter model possessing six semiconductor switching elements was designed and a switching algorithm was embedded into the inverter model. Inverter model and drive method will be described in Section 5.1, properly.

Table 3. m and r values in the studied motors

m	r	Motor structure
2/6	4/6	Hybrid A
4/6	2/6	Hybrid B

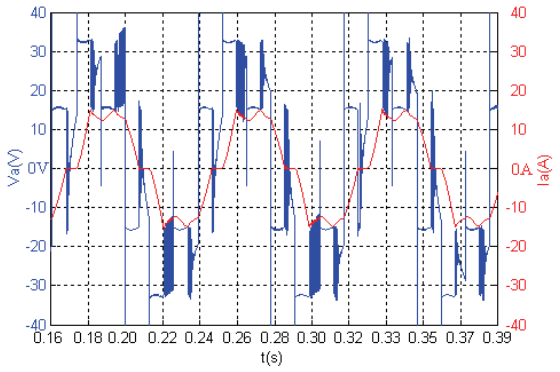

(a)

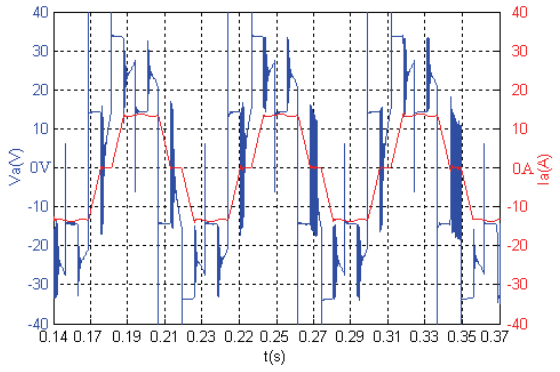

(b)

Fig. 4. Simulated phase voltage and current waveforms at 9Nm for two motor types (a) Hybrid A (b) Hybrid B

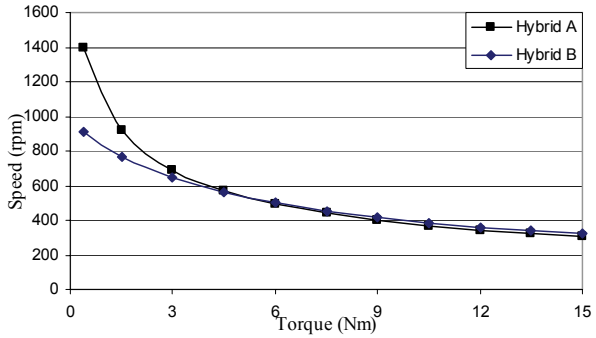

Fig. 5. Simulated speed versus torque curves of Hybrid A and Hybrid B

After completing the machine and inverter model, phase voltages were produced and hybrid motors were simulated at different load torques. Simulation results of phase voltage and current waveforms are given in Fig. 4 for Hybrid A and Hybrid B.

In the simulations, load torque is increased up to 15Nm step by step and speed versus torque curves are obtained

for two motor types. Simulated speed versus torque curves are shown in Fig. 5.

Since the hybrid motor structures consist of magnet and reluctance components, they can be considered as compound motors. It can be seen from Fig. 5 that speed versus torque curves of the hybrid motors resembles a compound DC motor characteristic. So the characteristics are among the characteristics of a permanent magnet DC motor and a DC series motor.

Because the amount of the reluctance component in Hybrid A is more than Hybrid B, the curve is more exponential and it resembles a DC series motor characteristic.

5. Experimental Study

5.1 Rotor prototypes, drive system configuration and drive method

After completing FE analysis and simulations, stator and rotor prototypes were built considering dimensions and specifications in Table 2. The photographs of the rotors and stator are given in Fig. 6.

The hybrid motor is needed to operate by a motor drive synchronized with the rotor position. The motor drive possesses two main parts. Power part consists of six N-channel MOSFETs and control part has a microcontroller, an EPROM and MOSFET drivers. Optic sensors are used for sensing the rotor position.

Drive method of the hybrid motor bases on the operation of a brushless DC motor (BLDC). Two phase windings are activated in each state, so the motor is operated with electrical 120° mode. Rotor position data should be transferred to the control system to energize the stator winding in proper duration. According to the position data, proper semiconductor elements are switched and a new position data is occurred when the rotor rotates by 60° electrical. This process continues periodically and rotor and stator magnetic flux are kept 90° electrical with respect to each other by modifying the stator current. Six switching states are occurred in one electrical round of the rotor.

In this operation, motor drive and position sensing system realizes the same function with the commutator and brushes in direct current machines. It can be said that electronically commutation takes the place of mechanically commutation by this method.

(a)

(b)

(c)

Fig. 6. The photographs of the motor: (a) Stator and motor body; (b) Hybrid A; (c) Hybrid B

5.2 Static torque experiments

For testing the motors, first, static torque experiments were realized in order to obtain the torque profiles of the hybrid motors. A test bench was used to measure the produced torque according to the rotor position. The test bench possesses a disc brake and a torque transducer. So, it makes it possible to lock the rotor and measure the static torque value at a rotor position. The photograph of the test bench and proposed motor is shown in Fig.7.

Rotor of the machine was locked by the disc brake, two stator windings were fed by a constant current value and the static torque value was measured and recorded. Then, the rotor was rotated by 5 mechanical degrees and the same procedure was repeated for one electrical round of the each hybrid rotor. All the process was also repeated for different β values for each hybrid rotor. Similar to FE simulations, in order to obtain the torque profiles for the BLDC operation mode, recorded values were shifted by electrically 60°. Measured torque profiles of the hybrid motors are shown in Fig. 8. It can be seen from Fig.2 and Fig.8 that FE analysis results and measured results are quite similar. However, the maximum values of simulated torque curves are higher than the measured values at 20A.

Static torque measurements were realized for 14 different β values and 5 different current values (5A, 10A, 20A, 30A, 40A and 50A). So, a lot of torque profiles occurred for the hybrid motors. Similar to FE study, T_{avg} and T_{max} values can be obtained from measured torque

Fig. 7. The photograph of the test bench and proposed motor

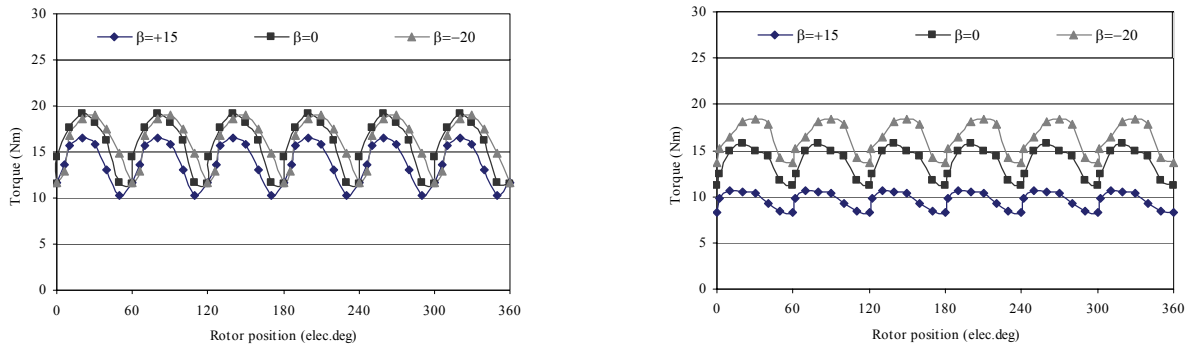

Fig. 8. Measured torque behaviors as a function of the rotor position for different β values in the (a) Hybrid A (b) Hybrid B (I=20A)

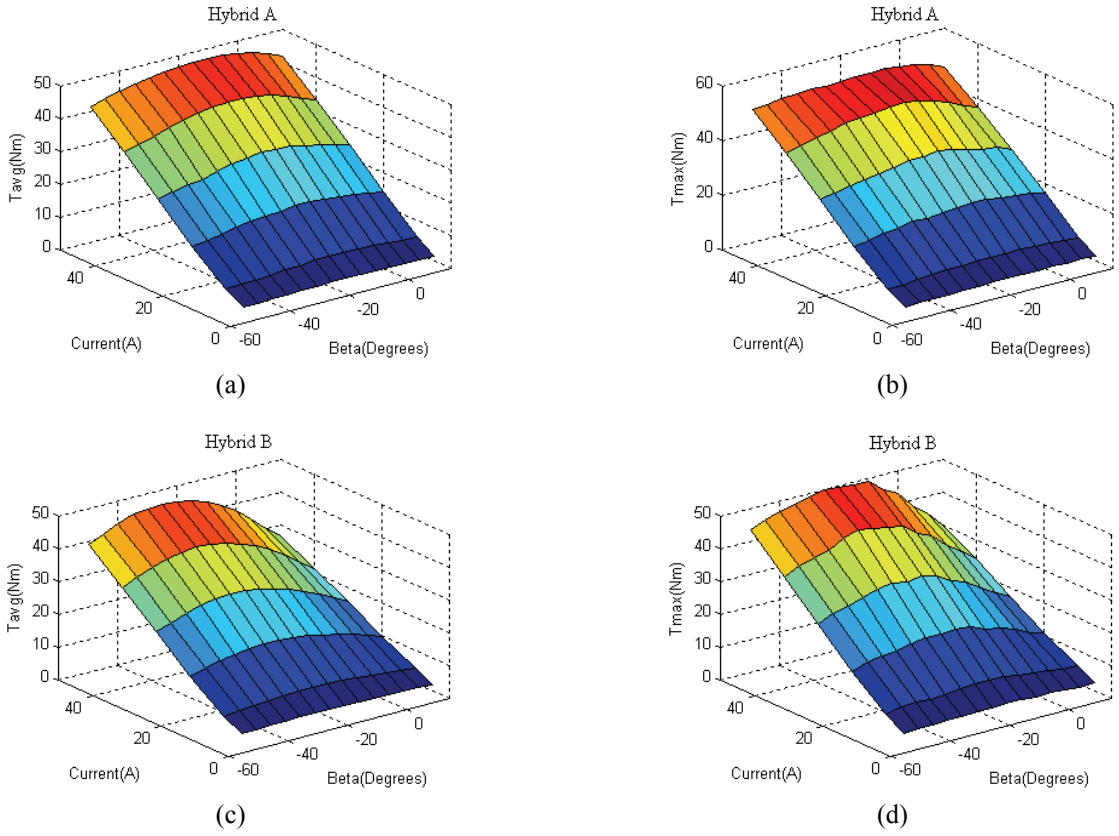

Fig. 9. Experimental results of T_{avg} (a), (c) and T_{max} curves (b), (d) as a function of β and current for Hybrid A and Hybrid B

profiles. In order to evaluate the experimental data together, 3-D graphs can be formed and T_{avg} and T_{max} values can be obtained related to variable β and current. Experimental T_{avg} and T_{max} curves are illustrated in Fig. 9 for Hybrid A and Hybrid B. Experimental results of T_{avg} and T_{max} values are quite similar to the analysis results in Fig. 3 at low current values. However, the measured values obtained lower than analysis results by the increase of the current. Although B-H curves of materials were defined in the FE software providing the curves of real materials used in the motor, there is a difference between analysis and experimental results, especially at high currents. Therefore, an advanced FE software can be used in order to include saturation effect completely. The difference may also arise from the elasticity of the disc brake.

It can be seen from Fig. 9 that at low currents T_{avg} and T_{max} values are not affected by β so much. However, the values considerably change by the variation of β at high current values. Acceptable β ranges can be determined experimentally according to the maximum values of T_{avg} and T_{max}.

Acceptable β ranges in Table 4 are wider than the values formed according to FE simulations. So, a common β value can be determined from FE results and Table 4. -20° was

Table 4. Acceptable β ranges for T_{avgmax} and T_{max} in the hybrid motors considering experimental study

Motor Type	T_{avgmax} β Range (Degrees)	T_{max} β Range (Degrees)
Hybrid A	-20˚ - 0˚	-20˚ - 0˚
Hybrid B	-30˚ - -10˚	-30˚ - -15˚

chosen as β for the load tests.

5.3 Load tests

After completing static torque experiments and determining the suitable β for the hybrid rotors, load tests were made on the test bench. The proposed motors were loaded by means of an auxiliary DC generator on the test bench. Measured phase voltage and current waveforms at 9Nm are given in Fig. 10.

Experimental speed versus torque curves were also obtained by loading the machines up step by step. The curves are shown in Fig. 11. Bus voltage can be chosen as 48 V and maximum load torque can be achieved as 13.5 Nm because of the features of the auxiliary machine.

Experimental curves are quite similar to the simulated curves in Fig. 5. However, simulated value of the speed is higher than the experimental value in Hybrid A at low load

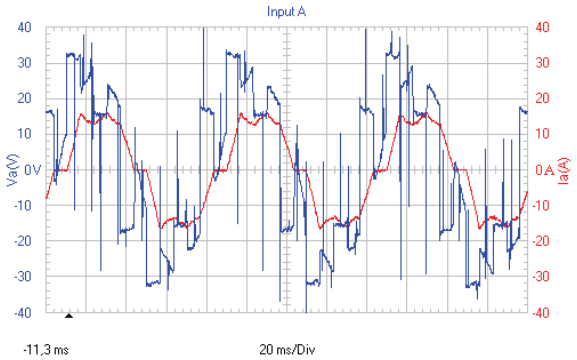

(a)

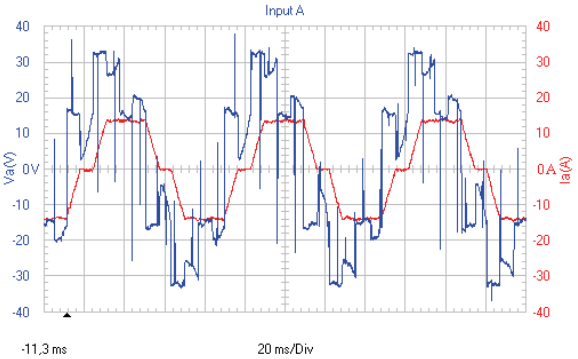

(b)

Fig. 10. Measured phase voltage and current waveforms at 9Nm for two motor types: (a) Hybrid A; (b) Hybrid B

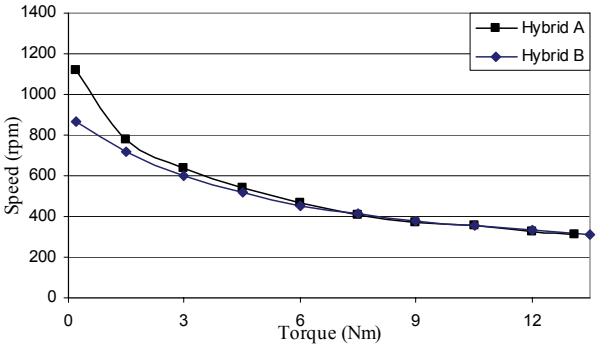

Fig. 11. Experimental speed versus torque curves of Hybrid A and Hybrid B

torques. In Hybrid A, reluctance percentage is more than Hybrid B, so machine flux is quite weak compared to Hybrid B. Due to the weak flux, motor speed reaches high values at low torque values. Therefore the difference between simulated and experimental values can be arisen that the sensibility of the torque transducer may be low and low torque values cannot be measured accurately or the transducer may cause some error in the measurement because of its calibration.

6. Conclusion

This paper presents a comparison of two rotor configuration considering the amount of magnet and reluctance components on the rotor. As a summary, rotor configurations were introduced; FE study was performed on the rotors; mathematical model of the motors were built and experimental tests were realized and compared to the simulation studies. The presentable results of the study are given as follows:

1) The proposed motor structure enables to configure and to compare several rotors having different hybridization.
2) The interaction between the magnet and reluctance torques can be investigated by changing the mechanical angle between the parts and suitable β value can be detected.
3) The amount of the reluctance part is more than the magnet part's in Hybrid A, in contrast Hybrid B possesses much magnet amount. So, Hybrid A and Hybrid B were compared considering the produced torques and speed versus torque curves.
4) FE study was performed in order to obtain T_{avg} and T_{max} depending on current and β values and β ranges were determined according to the FE results. β ranges are the same in Hybrid A and Hybrid B.
5) Mathematical models of the proposed motors were constituted, computer aided simulations were performed and loaded conditions were investigated.
6) Through the static torque measurements, produced

torque waveforms were obtained for different current and β values. T_{avg} and T_{max} surfaces were formed by experimental data. Experimental β ranges were determined. Experimental β ranges correspond to FE simulations but experimental ranges are wider than the simulated ones.

7) It was seen in both simulations and experimental study that the angle β became a significant parameter along with the increase of the current.
8) Experimental study was continued by the loaded tests. Phase voltage and current waveforms are very similar to the simulated waveforms. So, it proves the success of the mathematical model of the motors and inverter.
9) The simulated and experimental speed versus torque curves are also very similar, too. The hybrid motors can be defined as compound DC motors having different series and shunt windings considering the speed versus torque curves. The motors even can be named as brushless DC compound motors.

These results show that the proposed motor types can be used in different applications by modifying the magnet and reluctance parts and β according to the demand of the mechanical load.

Owing to show a compound DC characteristic, the unloaded speed is limited through the rotor flux in the hybrid motors. In addition, the loaded capacity of the hybrid motors is quite high. Eventually, usage of the proposed hybrid motors in electrical vehicles will be a suitable application area for this work.

References

[1] B. J. Chalmers, L. Musaba and D. F. Gosden, "Variable-frequency Synchronous Motor Drives for Electrical Drives", IEEE Transactions of Industry Applications, Vol.32, No.4, pp. 896-903, 1996.

[2] D.F. Gosden, B. J. Chalmers and L. Musaba, "Field weakening performance of a synchronous motor with two-part motor", 8th International Conference on electrical Machine and Drives, pp. 244-247, 1997, Cambridge, England.

[3] C. L. Gu, B. J. Chalmers and C. W. Lu, "Rotor design optimization of synchronous machine with two-part rotor", IEEE International Electric Machines and Drives Conference, pp. TB2/6.1 - TB2/6.3, 1997, Milwaukee, USA.

[4] B. J. Chalmers, R. Akmese and L. Musaba, "Design and Field Weakening Performance of Permanent-Magnet/Reluctance Motor with Two-Part Rotor", IEE Proc. Electr. Power Appl., Vol. 145, No. 2, pp. 133-139, 1998.

[5] B. J. Chalmers, R. Akmese and L. Musaba, "PM reluctance motor with two-part rotor", IEE Colloquium on New Topologies for Permanent Magnet Machines, pp. 6/1-6/5, 1997, London, England.

[6] W. L Soong and N. Ertugrul, "Field-Weakening Performance of Interior Permanent-Magnet Motors", IEEE Transactions of Industry Applications, Vol.38, No.5, pp. 1251-1258, 2002.

[7] P. Guglielmi, G. Giraudo, G.M. Pellegrino and A. Vagati, "PM assisted synchronous reluctance drive for minimal hybrid application", IEEE 39th IAS Annual Meeting, pp. 299-306, 2004, Seattle, USA.

[8] P. Niazi and H. A. Toliyat, "Design of a low-cost concentric winding permanent magnet assisted synchronous reluctance motor drive", IEEE 40th IAS Annual Meeting, pp. 1744-1748, 2005, Kowloon, Hong Kong.

[9] W. Guo and Z. Zhao, "Design and experiments of two-glued axially-laminated synchronous reluctance permanent magnetic motors", International Conference on Power Electronics and Drive Systems, pp.1374-1379, 2005, Kuala Lumpur, Malaysia.

[10] W. Guo, Z. Zhao and Y. Zhang, "Analysis and experimental study of slot effect in synchronous reluctance permanent magnet motors", International Power Electronics and Motion Control Conference pp. 1-6, 2006, Shanghai, China.

[11] P. Guglielmi, M. Pastorelli and A. Vagati, "Cross Saturation Effects in IPM Motors and Related Impact on Sensorless Control", IEEE Transactions on Industry Applications, Vol. 42, No.6, pp. 1516-1522, 2006.

[12] I. Boldea, C. I. Pitic, C. Lascu, G. -D Andreescu, L. Tutelea, F. Blaabjerg and P. Sandholdt, "DTFC-SVM Motion-Sensorless Control of a Pm-Assisted Reluctance Synchronous machine as Starter-Alternator for Hybrid Electric Vehicles", IEEE Transactions on Power Electronics, Vol. 21, No.3, pp. 711-719, 2006.

[13] P. Niazi, H. A. Toliyat, D. H. Cheong and J. C. Kim, "A Low-Cost and Efficient Permanent-Magnet-Assisted Synchronous Reluctance Motor Drive", IEEE Transactions on Industry Applications, Vol. 43, No. 2, pp. 542-550, 2007.

[14] H. W. Kock and M. J. Kamper, "Dynamic Control of the Permanent Magnet-Assisted Reluctance Synchronous Machine", IET Electr. Power Appl., Vol. 1, No. 2, pp. 153-160, 2007.

[15] S. Talebi, P. Niazi and H. A. Toliyat, "Design of a permanent magnet-assisted synchronous reluctance motors made easy", IEEE Industry Applications Conference, pp.2242-2248, 2007, New Orleans, USA.

[16] N. Bianchi, S. Bolognani, D. Bon and M. D. Pré, "Rotor Flux-Barrier Design for Torque Ripple Reduction in Synchronous Reluctance and Pm-Assisted Synchronous Reluctance Motors", IEEE Transactions on Industry Applications, Vol.45, No.3, pp. 921-928, 2009.

[17] R. Karimagako, M. H. Nagrial, and J. Rizk, "Analysis and design of permanent magnet assisted synchronous reluctance machines", 5th IET Inter-national

Conference on Power Electronics, Machines and Drives, pp.1-6, 2010, Brighton, England.

[18] M. Barcaro, N. Bianchi and F. Magnussen, "Permanent-Magnet Optimization in Permanent-Magnet-Assisted Synchronous Reluctance Motor for a Wide Constant-Power Speed Range", IEEE Transactions on Industrial Electronics, Vol. 59, No. 6, pp. 2495-2502, 2012.

[19] P. Guglielmi, B. Boazzo, E. Armando, G. Pellegrino and A. Vagati, "Permanent-magnet Minimization in PM-Assisted Synchronous Reluctance Motors for Wide Speed Range", IEEE Transactions on Industry Applications, Vol.49, No.1, pp. 31-41, 2013.

[20] E. Kandemir Beser, S. Camur, B. Arifoglu and E. Beser, "Application of a Four-Pole Hybrid Motor Structure Suitable for Modifying the Rotor Hybridization Ratio", International Review of Electrical Engineering, Vol. 5, No.5, pp.2049-2056, 2010.

[21] E. Kandemir Beser, S. Camur, B. Arifoglu and E. Beser, "Analysis and Application of a Hybrid Motor Structure Convenient to Modify the Magnet and Reluctance Torques on the rotor", Journal of Electrical Engineering & Technology, Vol. 7, No. 3, pp. 349-357, 2012.

Esra Kandemir Beser was born in Kocaeli, Turkey, on June 10, 1980. She received the B.S., M.S. and Ph.D. degrees in electrical engineering from Kocaeli University, Kocaeli, Turkey, in 2002, 2004 and 2013, respectively. Currently, she is an Assistant Professor with the Department of Electrical Engineering, Kocaeli University. Her research interests include design and analysis of electrical machines, brushless dc motors and drives, motor control, power electronics and multilevel inverters.

Sabri Camur was born in Adapazari, Turkey, on March 14, 1965. He received the B.S. and M.S. degrees in electrical engineering from Yildiz University, Istanbul, Turkey, in 1989 and 1991, respectively, and the Ph.D. degree from Kocaeli University, Kocaeli, Turkey, in 1998. Currently, he is an Assistant Professor with the Department of Electrical Engineering, Kocaeli University. His research interests are design and control of electrical machines, power electronics, multilevel inverters, reactive power compensation, solar energy and applications, electronics and industrial electronics.

Birol Arifoglu was born in Ksanti, Greece, on June 5, 1968. He received the B.S. degree in electrical engineering from Yildiz University, Istanbul, Turkey, in 1989, the M.S. degree from Istanbul Technical University, Istanbul, Turkey, in 1993 and the Ph.D. degree from Kocaeli University, Kocaeli, Turkey, in 1998. Currently, he is an Assistant Professor with the Department of Electrical Engineering, Kocaeli University. His research interests are in the areas of power electronics, dc-dc converters, inverters, automatic control and applications, PLC and SCADA applications, wind energy and industrial electronics and applications.

Ersoy Beser was born in Kocaeli, Turkey, on March 23, 1977. He received the B.S., M.S. and Ph.D. degrees in electrical engineering from Kocaeli University, Kocaeli, Turkey, in 2000, 2004 and 2009, respectively. Currently, he is an Assistant Professor with the Department of Electrical Engineering, Kocaeli University. His research interests are power electronics, multilevel inverters, electrical machines, motor control, microprocessors and PV systems.